JOURNAL OF MATERIALS SCIENCE 28 (1993) 1563–1572

Preparation and surface characterization of zincated aluminium memory-disc substrates

B. R. STROHMEIER*, W. T. EVANS, D. M. SCHRALL
Aluminum Company of America, Surface Technology Division, Alcoa Technical Center, 100 Technical Drive, Alcoa Center, PA 15069, USA

The surface compositions of CW66 aluminium alloy memory-disc substrates following commercial alkaline and acidic cleaning treatments and a commercial zincating treatment were investigated using the techniques of X-ray photoelectron spectroscopy, low-energy ion-scattering spectroscopy, secondary ion mass spectrometry, and scanning electron microscopy. The commercial treatments were performed on the disc substrates following diamond turning, or diamond turning followed by alumina-slurry polishing. Results indicated that alumina-slurry polishing of CW66 memory-disc substrates produces a slightly thicker and more hydrated aluminium oxide film compared to diamond-turned only discs. Commercial alkaline (Alprep 204) and acidic (Alprep 230) cleaners do not significantly affect the aluminium oxide composition nor thickness on CW66 alloy. These cleaning treatments also do not appear to significantly affect the amount of surface carbon contamination, nor the amounts of trace surface contaminants, such as sulphur and chlorine, that are present on the metal. Nitric acid stripping treatments performed between the first and second zincating treatments do not completely remove all of the first zincate film. A small amount of zinc remains on the disc surface. After removal of the first zincate film with nitric acid, SEM results showed that the first zincate treatment significantly roughened the aluminium substrate compared to the cleaned discs. The zincate films prepared in this study were discontinuous and consisted primarily of a $Zn(OH)_2/ZnO$ mixture on the surface and zinc metal in the bulk of the film. A variety of trace contaminants (i.e. sodium, silicon, sulphur, chlorine, potassium, calcium and iron) were also present in the zincate films. Some of these contaminants (i.e., sodium, chlorine and iron) most likely resulted from minor components in the zincating solutions. The others most likely resulted from inadvertent sample handling or from the adsorption of airborne contaminants prior to the analyses.

1. Introduction

Metallic coatings such as nickel are often applied to aluminium alloys by electrolytic or electroless deposition methods to enhance corrosion resistance, improve hardness and wear properties and to improve solderability [1]. Electroless nickel–phosphorus (Ni–P) coatings are also routinely used in the magnetic recording industry to improve adhesion between the magnetic media, typically cobalt–phosphorus (Co–P), and the aluminium alloy substrate (disc) [2]. Ni–P coatings are ideal for this purpose because of their favourable mechanical properties and because the electroless deposition of Co–P can be initiated directly on them [2]. However, electroless plating of aluminium alloys with Ni–P is usually very difficult to accomplish because the native oxide on aluminium surfaces prevents good adhesion between the aluminium substrate and the Ni–P film [1]. This native passivation oxide forms immediately (under ambient or aqueous conditions) on freshly created aluminium metal surfaces and is typically 4–5 nm thick [3–5]. To form an adherent Ni–P film on an aluminium substrate using electroless deposition techniques, an extensive series of chemical processing steps are normally required to replace the native oxide with a metallic film. Typically, the aluminium oxide film is replaced by immersion deposition of another metal which is resistant to oxidation. This metallic film, usually zinc, not only prevents the aluminium passivation oxide from forming again, but also provides a good metal-to-metal bond between the aluminium substrate and the electroless Ni–P deposit [1].

The most common method of applying the zinc film involves immersing the aluminium substrate into an alkaline zincate solution after appropriate cleaning

*Author to whom all correspondence should be addressed.

0022–2461

treatments [1]. A typical industrial processing sequence, referred to as the double zinc-immersion process, involves solvent cleaning, mild alkaline cleaning, rinsing, deoxidizing (mild acidic cleaning), rinsing, zincating for 30–60 s at room temperature, rinsing, removing the zinc film in 50% nitric acid, rinsing, and a final zincate treatment for 15–30 s at room temperature [1]. It has been reported that thin zinc films provide better corrosion resistance than thick films, and the double immersion process produces thinner, more uniform deposits than single immersion processes [1]. The exact formulations of commercial zincate solutions are usually proprietary, but they are known to contain zinc oxide, sodium hydroxide, chelating agents such as gluconates and tartrates, and various metal ions such as iron, nickel, lead and/or copper [1].

Zincate films are generally considered to be predominantly metallic [1]. However, the exact composition of such films is not well understood. Hence, this study was performed to obtain a better understanding of the nature of these films. This study involved the surface characterization of aluminium alloy (CW66) memory-disc substrates following commercial alkaline and acidic cleaning treatments and a commercial zincating treatment, which are typically performed to prepare the discs for electroless Ni–P deposition. The discs were analysed after each step in the zincating process. The surface analytical techniques of X-ray photoelectron spectroscopy (XPS or ESCA), low-energy ion-scattering spectroscopy (ISS) and secondary ion mass spectrometry (SIMS) were used to characterize the disc surfaces. In addition, the surface topography following each treatment was investigated by scanning electron microscopy (SEM).

2. Experimental procedure

2.1. Sample preparation

The memory-disc substrates used in this study were aluminium alloy CW66. This alloy is a higher purity version of the more common 5086 aluminium alloy and has a nominal composition of 4.0% Mg, 0.45% Mn and 0.15% Cr (remainder Al). Prior to zincate processing, the aluminium substrates were machined (diamond turned) on a lathe. The substrates were then polished using an aqueous alumina slurry. In this study, zincate treatments were performed on both the diamond-turned and the polished substrates for comparison.

TABLE I Zincate processing sequence for aluminium substrates[a]

1.	Mechanical machining of substrate
	(a) Diamond-turned only
	(b) Diamond-turned and slurry polished
2.	Alkaline cleaning (Alprep 204) for 5 min at 65 °C
3.	Acid cleaning (Alprep 230) for 2 min at 65 °C
4.	First zincate (Type 302) for 1 min at 25 °C
5.	50% nitric acid strip for 30 s at 25 °C
6.	Second zincate (Type 302) for 15 s at 25 °C

[a] Aluminium substrates were thoroughly rinsed with deionized water after each step.

All of the zincate processing steps were conducted with proprietary commercial solutions obtained from the Allied-Kelite (A-K) Division of Witco Chemical Corp., Los Angeles, CA. Alkaline and acidic cleaning were performed with Alprep 204 and Alprep 230 formulations, respectively. Zincate formulation Type 302 was used to perform the zincating treatments. All solutions were used according to the manufacturers' recommendations with respect to treatment times and conditions. The complete zincate processing sequence used in this study is listed in Table I.

2.2. ESCA analyses

ESCA spectra were obtained with a Kratos XSAM 800 photoelectron spectrometer equipped with a DS800 Control and Data System (Version V). All spectra were acquired using MgK_α radiation (1253.6 eV), with the anode operated at 15 kV and 15 mA. The hemispherical electron energy analyser was operated in the low-magnification, fixed retarding ratio (FRR) mode. ESCA survey spectra and narrow scan spectra were acquired using the medium resolution (retard ratio = 24) and high-resolution (retard ratio = 53) analyser modes, respectively. The instrument typically operates at pressures below 5×10^{-9} torr (1 torr = 133.322 Pa) in the analysis chamber. Samples were mounted on standard Kratos sample holders with double-sided tape.

All reported binding energies were referenced to the main C 1s line at 285.0 eV. Binding energies were measured with a precision of $\pm$ 0.1 eV. ESCA peak areas and peak synthesis routines (i.e. "curve fits") were determined using standard Kratos software. In all of the computations, the spectral background was assumed to be linear over the peak widths. Relative elemental sensitivity factors for quantitative determinations were calculated for the Kratos instrument according to the procedure described by Hanke *et al* [6]. The sensitivity factors used were: C 1s 0.79, O 1s 1.14, Al 2p 0.63, P 2p 1.24, S 2p 1.64, Cl 2p 2.07, Zn 2p3/2 0.81 (medium resolution, FRR analyser mode). Gaussian line shapes were used for the curve-fitting routines, except for the metallic component of the Al 2p peak envelopes. The Al 2p peak shape for clean aluminium metal is not Gaussian, but has a significant tail towards higher binding energies [7]. Hence, an experimental metallic Al 2p line shape obtained from a 99.999% Al sample, which had been sputter cleaned with argon, was used for curve-fitting purposes. The approximate aluminium oxide thicknesses on the disc samples were determined from the curve fits of the high-resolution Al 2p spectra using a uniform overlayer model described elsewhere [5]. The oxide thicknesses were determined with a precision of about $\pm$ 0.2 nm.

Commercial compounds for obtaining standard zinc ESCA spectra included ZnO (Fisher), $Zn(OH)_2$ (Alfa Products) and zinc foil (Alfa Products). $ZnAl_2O_4$ was prepared by mixing stoichiometric amounts of ZnO and γ-Al_2O_3 (Harshaw AL-1401P, 195 $m^2\ g^{-1}$) with a small amount of deionized H_2O and mulling into a paste. The paste was dried for 8 h at 110 °C,

finely ground, and subsequently calcined for 72 h at 900 °C. Formation of $ZnAl_2O_4$ was confirmed by X-ray diffraction analysis (XRD): No diffraction peaks characteristic of ZnO or γ-Al_2O_3 were observed.

2.3. ISS and SIMS analyses

ISS and SIMS spectra were obtained simultaneously with a 3M Model 525/610 ISS/SIMS spectrometer. $^4He^+$ ions were used as the primary ion beam. The primary ion-beam energy was 2 keV, with the beam rastered over a 0.5 mm^2 area. The specimen current was approximately 75 μA. During analysis, the pressure in the sample chamber was approximately 4×10^{-5} torr. Before analysis, typical base pressures of 5×10^{-9} torr or better were achieved.

2.4. SEM analyses

Secondary electron images were obtained with an ISI scanning electron microscope, Model 40. The electron beam energy was 15 kV.

3. Results and discussion

3.1. Aluminium cleaning treatments

Scanning electron micrographs of the diamond-turned and polished substrates, as-prepared and following the alkaline (Alprep 204) and acidic (Alprep 230) cleaning treatments, are shown in Fig. 1. For the diamond-turned discs, the cleaning treatments etch and roughen the disc surface. The polished substrates appeared slightly rougher than the diamond-turned substrates, in all cases.

The approximate surface compositions of the as-received and cleaned substrates (as determined by ESCA) are listed in Table II. The major elemental surface components on all of the samples were aluminium, oxygen and carbon, as would be expected. Small amounts (i.e. ~0.2–1 at %) of sulphur and chlorine contamination were also detected on most of the samples. Small amounts (i.e. ~1–2 at %) of phosphorus were detected on all of the cleaned samples. This result indicates that the cleaning solutions contain some type of phosphorus species, which leaves a residue on the aluminium oxide surface. The binding energies of the S 2p, Cl 2p and P 2s peaks were 169.8, 199.3 and 191.8 eV, respectively. These values are characteristic of sulphates, chlorides and phosphates, respectively [8]. Because sulphur and chlorine were detected both before and after the cleaning treatments, it appears that the Alprep 204 and 230 cleaners do not effectively remove these species from aluminium surfaces. However, the sulphur and chlorine detected may simply represent airborne contaminants, which adsorbed on the samples after the cleaning treatments. In any case, the amounts of these species on the disc surfaces were relatively small.

In general, the results shown in Table II indicate that the surfaces of the polished samples had lower amounts of carbon contamination present compared to the diamond-turned samples. However, the surface carbon concentration did not appear to be significantly affected by the cleaning treatments. This result indicates that both the alkaline and the acidic cleaners did not effectively remove hydrocarbon contamination from the discs. The polished samples also had somewhat higher amounts of oxygen present (relative to aluminium), compared to the diamond-turned samples. This result suggests that the surfaces of the polished samples were hydrated to a greater extent than the diamond-turned samples (i.e. $Al(OH)_3$ or AlOOH versus Al_2O_3. This finding is consistent with the fact that the polished samples were prepared in an alumina/water slurry.

TABLE II Approximate surface compositions (at %) determined by ESCA[a]

Sample treatment[b]	C	O	Al	P	S	Cl
DT as-received	37.8	34.9	26.5	ND[c]	0.7	0.2
DT Alprep 204	44.7	32.6	20.4	1.2	0.9	0.2
DT Alprep 204/230	36.1	38.1	23.9	0.8	0.8	0.2
P As-received	25.8	48.9	24.6	ND	0.8	ND
P Alprep 204	28.0	40.2	28.5	2.9	1.3	ND
P Alprep 204/230	29.3	43.1	25.3	1.0	1.0	0.3

[a]Atomic concentrations were determined from the appropriate ESCA peak areas and elemental sensitivity factors (see Section 2).
[b]DT, diamond turned; P, polished. For further details on cleaning treatments, see Table I.
[c]ND, not detected.

Fig. 2 shows the high-resolution Al 2p ESCA spectra obtained for the diamond-turned and polished substrates, as-prepared and following the alkaline and acidic cleaning treatments. In all cases, two peaks were evident in the spectra. The peak at lower binding energy is characteristic of aluminium metal, whereas, the peak at higher binding energy is characteristic of aluminium oxide and/or hydroxide [5]. The surfaces of aluminium materials are always oxidized and hydrated to various extents and it is impossible to distinguish between the various types of aluminium oxide and hydroxide by the Al 2p binding energy alone. A typical computer curve fit of an Al 2p spectrum, showing the oxidic and metallic components, is shown in Fig. 3.

The average oxidic and metallic Al 2p binding energies obtained for the samples were 74.6 and 71.5 eV, respectively. The O 1s spectra obtained for the samples could be fit to two peaks corresponding to aluminium oxide (531.6 eV) and aluminium hydroxide (532.9 eV). The Al 2p and O 1s binding energies obtained for the samples did not vary by more than 0.2 eV from the above values, which is within the experimental error of the measurement. These results indicate that the oxide composition was similar in all cases. The average Al 2p and O 1s binding energies were also similar (i.e. within 0.2 eV) to values previously reported for the passivation oxide films formed on other aluminium alloys [5, 9, 10].

As mentioned above, the O 1s peaks could be fit to both an oxide and hydroxide component, which is consistent with previous studies [5, 9, 10]. The relative O 1s hydroxide/oxide peak intensity ratio can be used to measure the relative extent of surface hydration

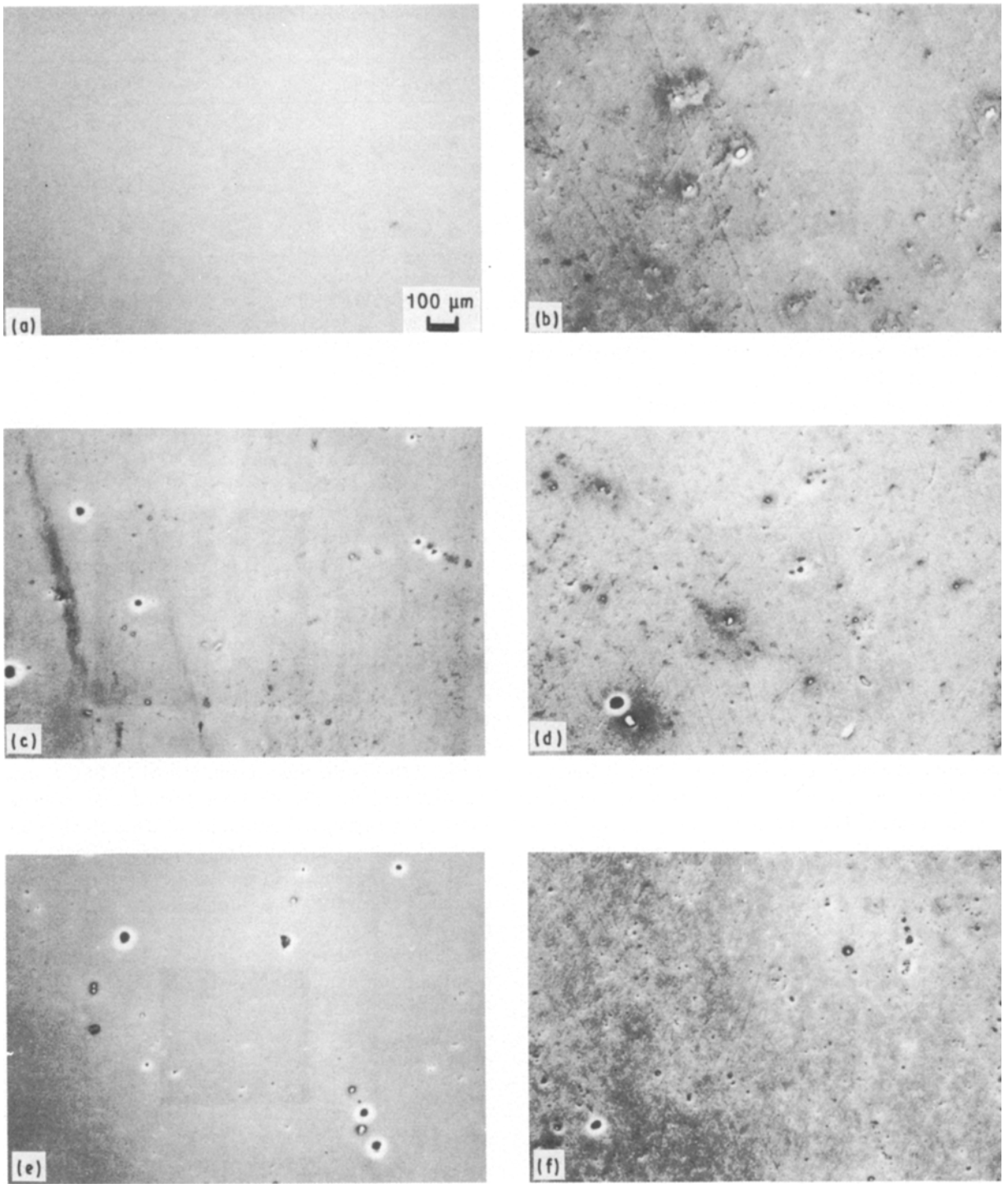

Figure 1 Scanning electron micrographs of pretreated (a, c, e) diamond turned and (b, d, f) polished aluminium substrates. (a) As-turned, (b) as-polished, (c, d) dipped for 5 min in AK 204 at 65 °C, (e, f) additional dip for 2 min in A-K 230 at 65 °C.

present on aluminium oxide films [9, 10]. The O 1s hydroxide/oxide intensity ratios obtained for the samples are listed in Table III which shows that, in general, the polished samples had slightly more aluminium hydroxide present than did the diamond-turned samples, although these differences were small. This finding is consistent with the surface composition results discussed above.

The Al 2p oxide/metal intensity ratio varied somewhat between the samples, as shown in Fig. 2. The relative peak intensities (areas) of the oxidic and metallic peaks are a function of the thickness of the oxide and hydroxide layers [5]: the thicker the oxide, the greater is the relative oxide/metal intensity ratio. The approximate oxide thickness can be estimated from the relative peak areas of the oxidic and metallic Al 2p peaks, as determined by computer curve fitting (see Fig. 3) [5].

The oxide thicknesses calculated for each sample are listed in Table IV which also shows the oxide thicknesses determined by ISS depth profiling. The Al_2O_3 sputter rate during the ISS depth profiles was determined by profiling a 20 nm anodic Al_2O_3/Al standard that was prepared by a previously described method [11]. In all cases, the oxide thicknesses determined by ESCA and ISS agreed within $\pm$ 0.1–0.4 nm.

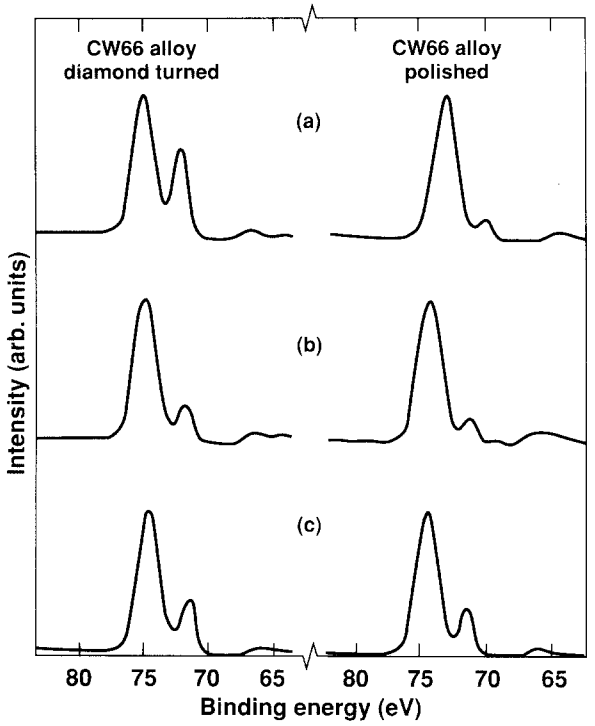

Figure 2 Comparison of the Al 2p ESCA spectra obtained for diamond-turned and polished CW66 alloy: (a) as-received, (b) Alprep 204/230 cleaned, (c) Alprep 204/230 cleaned.

TABLE III O 1s hydroxide/oxide relative ESCA intensity ratios[a]

Sample treatment[(b)]	O 1s hydroxide/oxide
CW66 DT as-received	0.35
CW66 DT Alprep 204	0.59
CW66 DT Alprep 204/230	0.41
CW66 P as-received	0.51
CW66 P Alprep 204	0.62
CW66 P Alprep 204/230	0.54

[a]O 1s hydroxide/oxide relative ESCA intensity ratios were determined by computer curve fitting the O 1s peak envelopes with hydroxide and oxide components and ratioing the respective peak areas.
[b]DT, diamond-turned aluminium blank; P, polished aluminium blank. For further details on cleaning treatments, see Table I.

TABLE IV Oxide thickness determined by ESCA and ISS oxide thickness (nm)

Sample treatment[a]	ESCA	ISS
DT as-received	2.6	2.8
DT Alprep 204	4.0	3.9
DT Alprep 204/230	3.2	3.3
P As-received	4.8	4.5
P Alprep 204	4.4	4.0
P Alprep 204/230	3.6	3.4

[a]DT, diamond turned; P, polished. For further details on cleaning treatments, see Table I.

The results shown in Table IV indicate that the untreated polished sample had a slightly thicker oxide than did the untreated diamond-turned sample. Because the polished samples were prepared in an alumina/water slurry, the observed increase in the overall

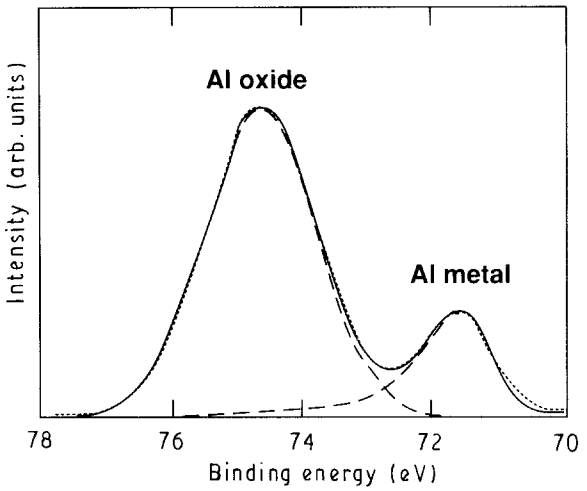

Figure 3 Curve fit for an Al 2p ESCA spectrum: CW66 alloy, diamond-turned, Alprep 204/230 cleaned. (- - -) Component peaks, (—) synthetic envelope, (· · ·) experimental data.

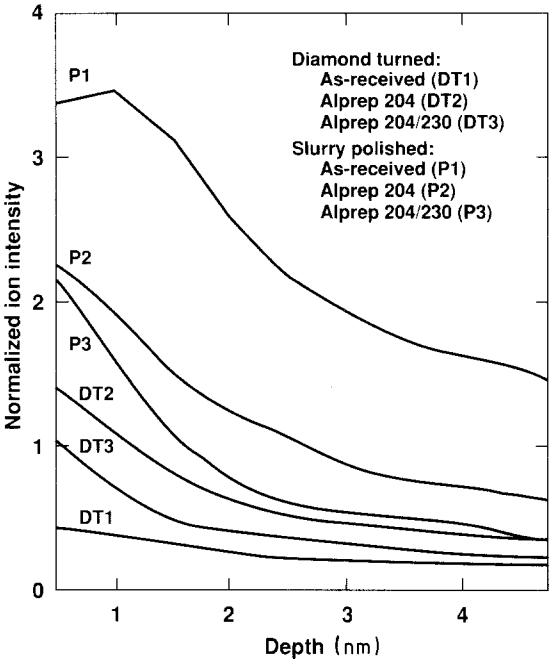

Figure 4 SIMS depth profiles for $AlOH^+$.

oxide thickness is most likely the result of increased aluminium hydroxide formation on the polished specimens. The observed increase in the oxide thickness is consistent with the surface composition and the O 1s curve fitting results discussed earlier, which both indicated that the polished samples were hydrated to a greater extent than the diamond-turned samples. This argument was further supported by SIMS depth profiles obtained for the samples for $AlOH^+$ ions (normalized to the Al^+ signal intensity). The normalized $AlOH^+$ signal intensity should be a valid measure of the relative amount of aluminium hydroxide present on the sample surfaces. Fig. 4 shows that the normalized $AlOH^+$ signal intensity was greatest on the polished samples. In any case, the observed differences in oxide thickness between the cleaned samples were relatively small (i.e. 0.5–1.0 nm). Hence, it appears that

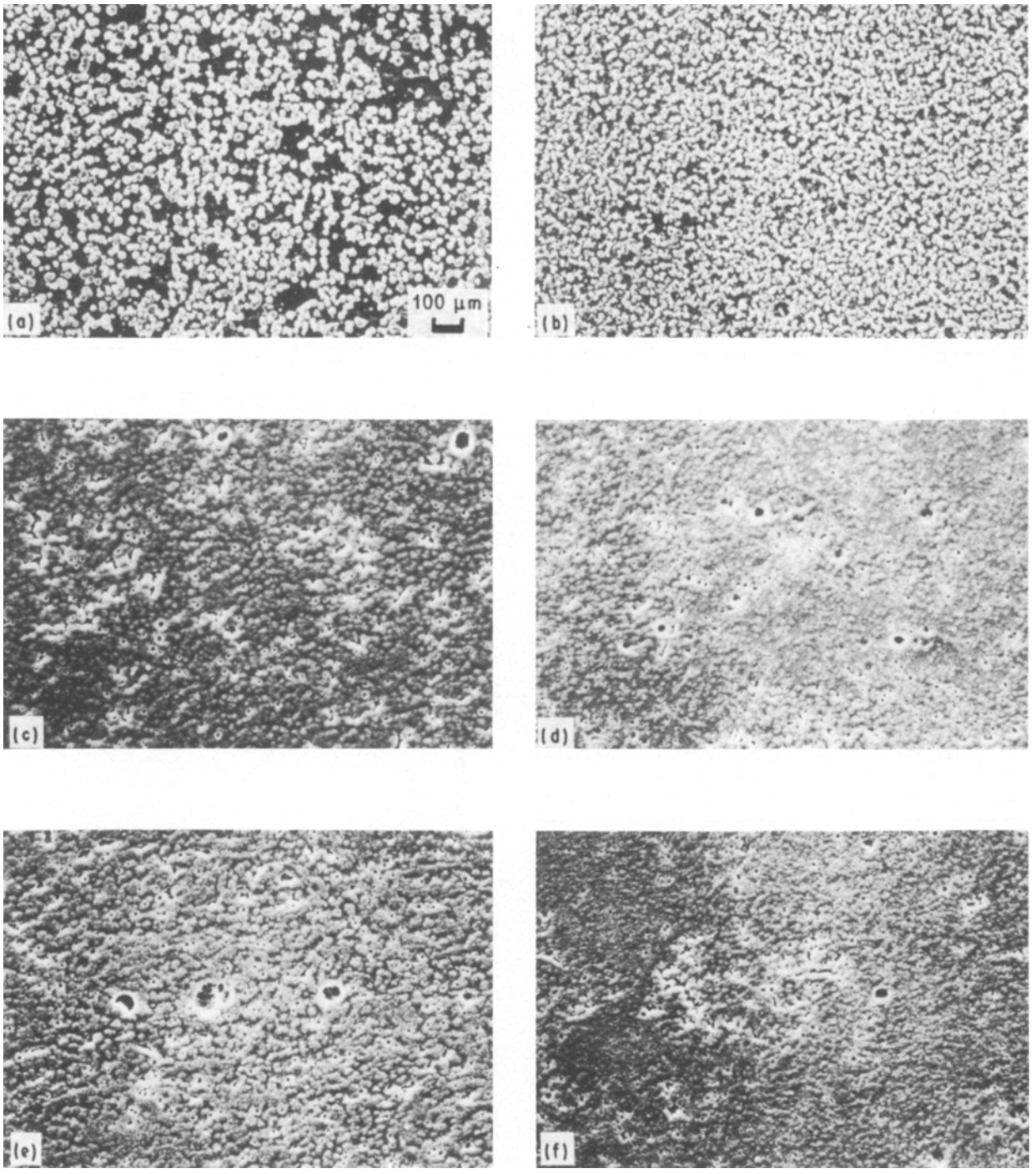

Figure 5 Scanning electron micrographs of zincate films on (a, c, e) diamond-turned and (b, d, f) polished aluminium substrates. (a, b) 60 s dip in A-K 302 at 25 °C, (c, d) 30 s dip in 50% HNO_3 at room temperature, (e, f) 15 s dip in A-K 302 at 25 °C.

the alkaline and acidic cleaners do not significantly affect the overall oxide thickness on the discs. Most likely, these cleaners do remove some of the initial oxide, but during rinsing and subsequent exposure to air, similar oxide thicknesses are reformed on the metal (i.e. passivation oxides.)

3.2. Zincate processing

Scanning electron micrographs of the cleaned diamond-turned and polished substrates following the first zincate, nitric acid strip and second zincate processing steps (see Table I) are shown in Fig. 5. Following the first zincate treatment, the surface of the diamond-turned substrate did not appear as uniform as that of the polished substrate. However, after the second zincate treatment, no significant differences in surface topography were observed between the two substrates. Following the 50% nitric acid stripping treatment, the surfaces of both substrates appeared significantly rougher than the cleaned substrates (see Figs 1 and 5). This roughness is caused by the alkaline (i.e. ~2509 NaOH l^{-1}) first zincate treatment. Aluminium metal would be dissolved in the zincate solution, roughening the surface. The subsequent nitric acid

treatment removes the first zincate layer, revealing the roughened aluminium substrate underneath.

The approximate surface compositions of the zincated and nitric acid stripped substrates, as determined by ESCA, are listed in Table V, which shows that the major elemental surface components on the zincated discs were, as would be expected, carbon, oxygen and zinc. Small amounts (i.e. ~2–5 at %) of aluminium were also detected on the discs following the zincating treatments (first and second). High-resolution ESCA spectra of the Al 2p region for the zincated discs showed both oxidic and metallic components, with an indicated aluminium oxide thickness of ~40–45 nm. These results indicate that the zincate films were either discontinuous, with exposed aluminium areas showing, or the zincate films were thinner than the sampling depth of ESCA, which would allow the underlying aluminium substrate to be detected. The scanning electron micrographs shown in Fig. 5 indicate that the former case was true. ISS and SIMS depth-profiling results indicated that the thicknesses of the first and second zincate films were about 25–30 nm and 10 nm, respectively. This difference results from the different zincating times (i.e. 60 and 15 s, respectively).

On the 50% nitric acid stripped discs, the major elements detected by ESCA were carbon, oxygen and aluminium (see Table V). However, small amounts (i.e. ~0.5–0.6 at %) of zinc were also detected on the nitric acid stripped discs, which indicates that the stripping treatment does not completely remove all of the first zincate film. The aluminium oxide thickness on the nitric acid stripped discs was found to be about 4.3 nm for both the polished and the diamond-turned substrate. The 50% nitric acid solution does not dissolve the initial aluminium oxide film to any significant extent.

TABLE V Approximate surface compositions (at %) determined by ESCA[a]

Sample treatment[b]	C	O	Al	S	Cl	Zn
DT 1st zincate	43.6	40.2	4.7	1.0	ND[c]	10.5
DT 50% HNO_3 strip	41.4	34.4	21.8	1.7	0.2	0.5
DT 2nd zincate	60.7	23.9	3.6	0.5	0.3	11.0
P 1st zincate	54.3	30.2	1.9	0.9	0.1	12.6
P 50% HNO_3 strip	40.4	35.3	22.0	1.5	0.3	0.6
P 2nd zincate	49.2	32.5	5.2	1.2	0.3	11.6

[a]Atomic concentrations were determined from the appropriate ESCA peak areas and elemental sensitivity factors, (see Section 2).
[b]DT, diamond turned; P, denotes polished. For further details on zincate treatments, see Table I.
[c]ND, not detected.

Small amounts (~0.2–2 at %) of sulphur and chlorine were also detected by ESCA on both the zincated and the nitric acid stripped discs (see Table II). High-resolution ESCA spectra indicated that these contaminants were present as sulphates and chlorides, respectively. ISS and SIMS, which have lower detection limits than ESCA, indicate that sodium, silicon, potassium, calcium and iron were also typical contaminants present on the zincated discs. Typical ISS and SIMS spectra for a zincated disc (diamond-turned, first zincate) are shown in Fig. 6. (Note the intense Na^+ peak observed in the SIMS spectrum is not shown in Fig. 6 for clarity.) These surface contaminants presumably arise from minor components present in the proprietary zincating solutions. Because sodium, silicon, potassium, calcium and iron could not be detected by ESCA, these species were present in amounts below ~0.1 at %. Although the amounts of these contaminants were relatively low, it should be noted that the zincated and nitric acid stripped samples all had relatively high amounts of surface carbon present (i.e. ~40–60 at %).

High-resolution ESCA spectra of the Zn 2p3/2, O 1s and the X-ray-induced Zn *LMM* Auger lines were obtained for the zincated discs. Strohmeier and Hercules have studied the ESCA spectra for a variety of zinc compounds [12]. Fig. 7 shows typical ESCA spectra of the Zn 2p3/2 and Zn *LMM* Auger lines for zinc metal, ZnO and $ZnAl_2O_4$. The Zn 2p3/2 line is a singlet, which shows relatively small chemical shifts between different zinc species (see Fig. 7). For example, the typical chemical shifts reported in the literature

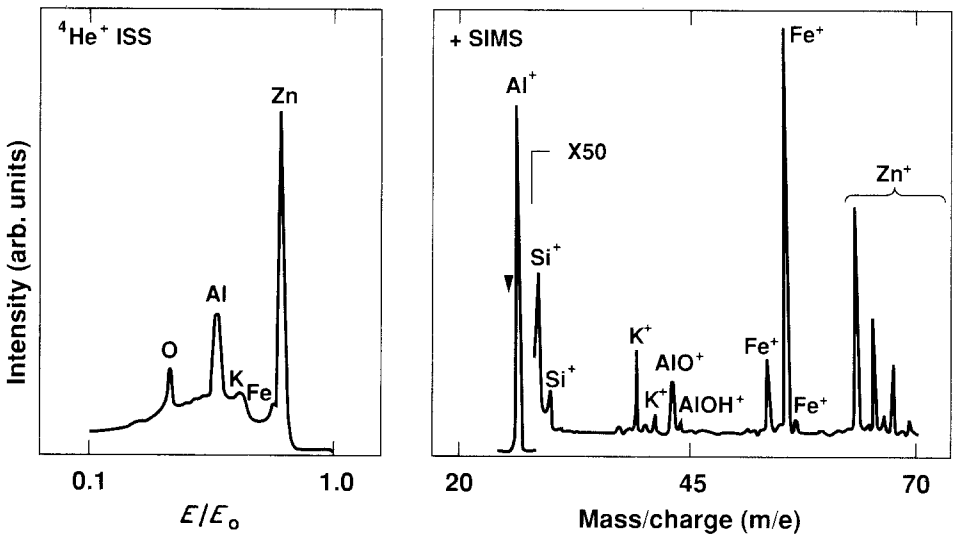

Figure 6 (a) ISS and (b) SIMS spectra obtained for CW66 alloy (diamond-turned) after first zincate treatment.

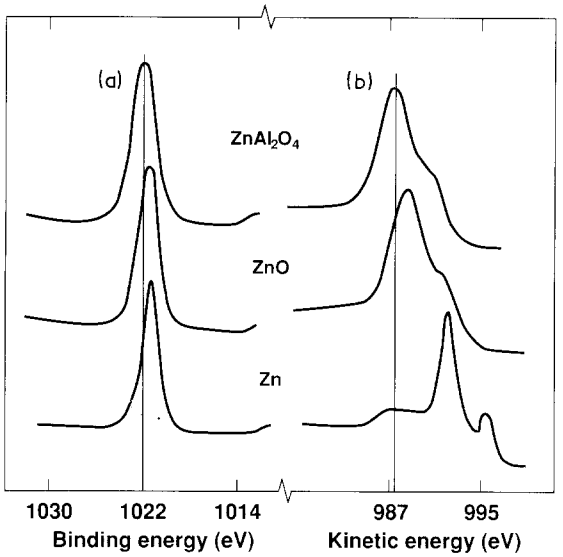

Figure 7 ESCA spectra of the (a) Zn 2p3/2 and (b) Zn *LMM* Auger lines for various zinc reference compounds (reproduced from [12] with permission).

between the Zn 2p 3/2 lines of zinc metal and ZnO range between 0 and 0.3 eV [12–14]. In this study, a chemical shift of 0.2 eV was found between the Zn 2p3/2 lines of zinc metal and ZnO. Such small chemical shifts make the distinction between zinc metal and ZnO essentially impossible based on the Zn 2p3/2 binding energy alone. However, the X-ray-induced *LMM* Auger lines of zinc metal and ZnO are separated by ~ 3.5 eV and have very different shapes, allowing easy distinction between the two (see Fig. 7). Zinc *LMM* Auger bands consist of two peaks, although they are poorly resolved for Zn^{2+} species compared to zinc metal [12,13]. This is illustrated in Fig. 7 for ZnO and $ZnAl_2O_4$. The origin of the doublets is believed to arise from 1-s coupling [13]. The line widths for zinc metal are narrower than that observed for $Zn^{2=}$ species because of different transition probabilities and lifetimes in the final state [13].

Strohmeier and Hercules [12] found that the most convenient method for determining the chemical state of zinc using ESCA was to use the Auger parameter method originally described by Wagner *et al.* (i.e. Auger parameter = α = kinetic energy of the major Auger line minus the kinetic energy of the major photoelectron line for the element of interest [8,15]. In this study, the modified Auger parameter method [8] (i.e. modified Auger parameter = α' = binding energy of the major photoelectron line plus the kinetic energy of the major Auger line for the element of interest) was used to determine the chemical state of zinc on the discs. The modified Auger parameter is equal to the sum of the original Auger parameter and the energy of the excitation source (i.e., $\alpha' = \alpha + h\nu$). The modified Auger parameter is independent of the excitation energy and is more useful and convenient when making comparisons among data obtained from different instruments. The modified Auger parameter method has a major advantage over direct binding energy measurements. Because the separation between two lines is being measured, charge referencing is not necessary because static charge corrections cancel [8,15]. Hence, problems with choosing a particular line and binding energy value for reference purposes are eliminated.

TABLE VI Zinc Auger parameters for zincated aluminium substrates and standard zinc compounds

Sample treatment[a]	Zinc Auger parameter (eV) [(b)]
DT 1st zincate	2010.1
DT 2nd zincate	2010.1
P 1st zincate	2010.2
P 2nd zincate	2010.1
ZnO	2010.3
$Zn(OH)_2$	2009.9
$ZnAl_2O_4$	2009.9
Zn (metal)	2013.8
Zn (metal heated in air at 300°C for 4 h)	2010.3

[a]DT, diamond turned; P, denotes polished. For further details on zincate treatments, see Table I.
[b]Zinc Auger parameter = binding energy Zn 2p 3/2 + kinetic energy Zn *LMM*.

The modified Auger parameter values were determined for the zincated discs and a variety of standard zinc compounds (see Table VI). The standard compounds that were analysed included ZnO, $Zn(OH)_2$, $ZnAl_2O_4$ and zinc metal (both sputter-cleaned and heated in air). Table VI shows that the modified Auger parameters obtained for ZnO and the heated zinc metal were identical and these values differed from that of clean zinc metal by 3.5 eV, which is in excellent agreement with the shift reported in the literature (3.3 eV) [12]. It was found that the α' values for $Zn(OH)_2$ and $ZnAl_2O_4$ were identical and differed from the value obtained for ZnO by only 0.4 eV. This difference is relatively small and makes distinction between ZnO and $Zn(OH)_2$ and/or $ZnAl_2O_4$ difficult, based on the α' values alone.

Table VI shows that the α' values obtained for the zincated discs were between the values obtained for ZnO and $Zn(OH)_2$. This result suggests the possibility of a mixture of the two species. However, these observed differences were small and of the order of the typical experimental error for such measurements. (Note: as discussed above, the α' values for $Zn(OH)_2$ and $ZnAl_2O_4$ were identical. However, $ZnAl_2O_4$ is normally formed only at high temperatures (> 900 °C) [12]. The α' value for $ZnAl_2O_4$ was included in Table VI for information only.)

Although the modified Auger parameters obtained for the zincated discs could not positively distinguish between ZnO and $Zn(OH)_2$, the Zn *LMM* spectra obtained for the first zincated discs (both diamond-turned and polished) indicated that these discs had a small amount of zinc metal present on their surfaces, in addition to the oxidic zinc species. This finding is illustrated in Fig. 8a, which shows the Zn *LMM* spectrum obtained for the diamond-turned disc following the first zincating treatment. Two small shoulders, characteristic of zinc metal, are evident on the high kinetic energy side of the main oxidic peak (cf. Figs 7 and 8a). After the second zincating treatment, no metallic zinc peaks were evident in the Zn *LMM* spectra for either substrate (i.e. diamond-turned or

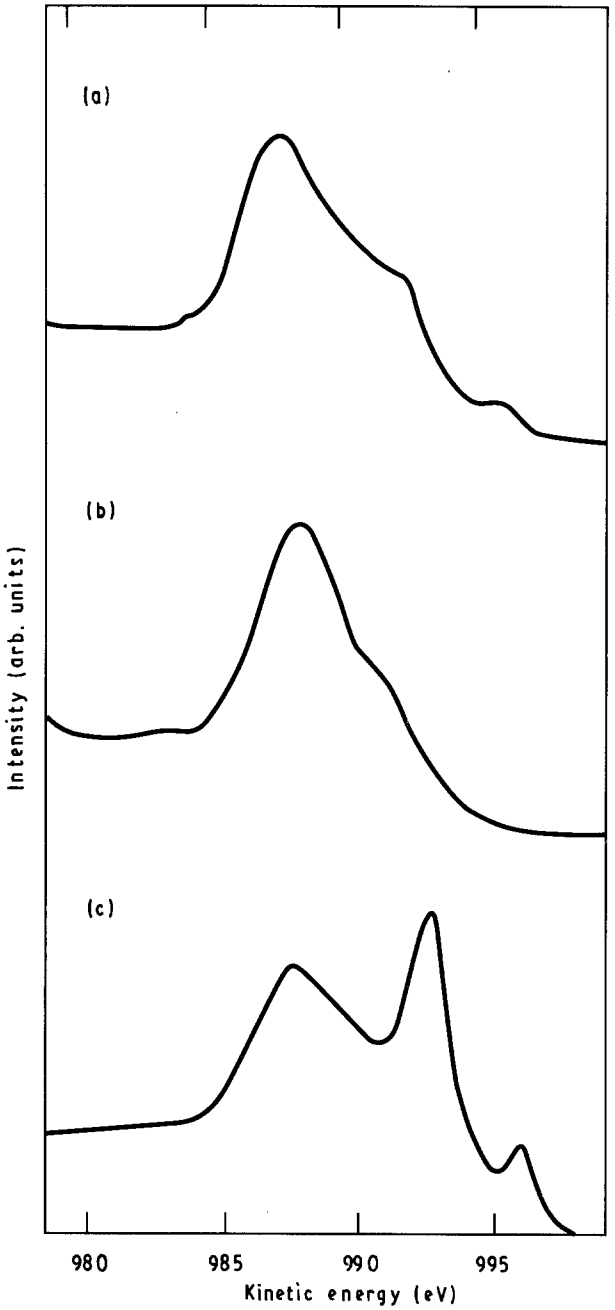

Figure 8 Zn *LMM* ESCA spectra obtained for zincate (Type 302) coated CW66 alloy (diamond-turned) : (a) first zincate, (b) second zincate, (c) second zincate after argon sputtering.

polished). A typical spectrum for a diamond-turned substrate following the second zincating treatment is shown in Fig. 8b. The only peaks seen in the spectrum are characteristic of oxidic zinc species. However, after 5 min, Ar^+ sputtering ($\sim$5 nm), metallic zinc peaks were clearly evident in the Zn *LMM* spectrum (see Fig. 8c). In all cases, metallic zinc was detected after Ar^+ sputtering (i.e. first and second zincate treatment, diamond-turned and/or polished substrate).

The detection of zinc metal in zincate films is not surprising, because the zincating process involves the anodic dissolution of aluminium and the cathodic deposition of zinc metal [1]. The overall electroless deposition process is as follows [1].

1. Dissolution of aluminium (anodic):

$$2Al^0 + 6OH^- \rightarrow 2Al^{3+} + 6OH^- + 6e^-$$
$$E^0 = 2.31\,V \qquad (1)$$

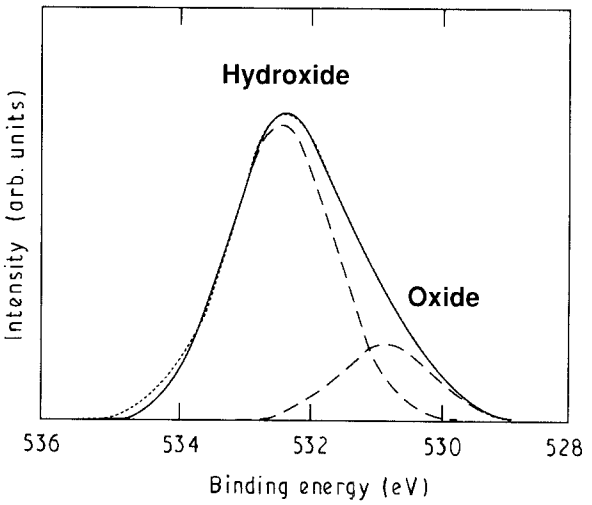

Figure 9 Curve fit for an O 1s ESCA spectrum: CW66 alloy, diamond-turned, Alprep 204/230 cleaned, after second zincate treatment (Type 302). (- - -) Component peaks, (—) synthetic data, (···) experimental data.

2. Deposition of zinc (cathodic):

$$3Zn(OH)_4^{2-} + 6e^- \rightarrow 3Zn^0 + 12OH^-$$
$$E^0 = -0.763V \qquad (2)$$

3. Overall reaction:

$$2Al^0 + 3Zn(OH)_4^{2-} + 6OH^- \rightarrow 2Al^{3+} + 3Zn^0 + 18OH^-$$
$$E^0 = 1.547\ V \qquad (3)$$

The metallic zinc film, which is deposited on the disc surface, would readily oxidize in air and/or the basic zincate solution, to form ZnO and/or $Zn(OH)_2$ on the surface of the zinc film. Hence, the ESCA results indicate that the zincate films prepared in this study consisted primarily of an oxidic zinc species (either ZnO or $Zn(OH)_2$) on the outer surface and zinc metal within the film.

As discussed above, the modified zinc Auger parameters could not readily distinguish between ZnO and $Zn(OH)_2$. However, the O 1s spectra obtained for the samples showed that in all cases, the zincate films consisted of a mixture of $Zn(OH)_2$ and ZnO that was predominantly hydroxide. The O 1s spectra for all of the zincated samples could be fit to two components, one at 530.6 $\pm$ 0.1 eV and the other at 532.3 $\pm$ 0.1 eV. These values correspond to the O 1s values obtained for the ZnO and $Zn(OH)_2$ standards, respectively. (Note: the experimental O 1s binding energy for Al_2O_3 was 531.6 $\pm$ 0.1 eV. Hence, a small contribution to the overall O 1s peak envelope might be present at this binding energy, as a result of the exposed aluminium substrate. This contribution, however, should be relatively small.) Fig. 9 shows a typical O 1s spectrum and computer curve fit for a zincate film (second zincate, diamond-turned substrate). In all cases (i.e. first and second and zincates for both substrates), the hydroxide component of the O 1s peak was dominant. The O 1s hydroxide/oxide relative intensity ratios ranged between 2.1 and 2.8 for the various samples.

The experimental O/Zn atomic ratios obtained for the ZnO, $Zn(OH)_2$ and $ZnAl_2O_4$ standards were 1.3, 2.2 and 4.3, respectively. These values are in reasonable agreement with the expected values and indicate that the relative ESCA elemental sensitivity factors used in this study were reasonably accurate. The O/Zn atomic ratios for the zincated discs ranged between 2.2 and 3.8, with an average value of 2.6 ± 0.4. These values are slightly higher than that obtained for bulk $Zn(OH)_2$, but definitely indicate that the zincate films are different from ZnO. The somewhat higher O/Zn atomic ratios obtained for the zincated discs can be attributed to the fact that not all of the oxygen detected was bound to zinc. Some of the oxygen was bound to the carbon contamination, the exposed aluminium substrate, and the trace contaminants that were detected. In any case, these results indicate that the zincate films prepared in this study consisted of a mixture of ZnO, $Zn(OH)_2$ and zinc metal.

4. Conclusion

1. Alumina-slurry polishing of CW66 memory-disc substrates produces a slightly thicker and more hydrated aluminium oxide film compared to diamond-turned only discs.

2. Commercial alkaline (Alprep 204) and acidic (Alprep 230) cleaners do not significantly affect the aluminium oxide composition or oxide thickness on CW66 alloy. These cleaning treatments also do not appear to affect significantly the amount of surface carbon contamination or the amounts of trace surface contaminants, such as sulphur and chlorine that are present on the metal.

3. Nitric acid stripping treatments performed between the first and second zincating treatments in commercial processes do not completely remove all of the first zincate film. A small amount of zinc (~ 0.5 at %) remains on the disc surface. After removal of the first zincate layer with the nitric acid solution, SEM showed that the first zincate treatment significantly roughened the aluminium substrate.

4. A variety of trace contaminants (i.e. sodium, silicon, sulphur, chlorine, potassium, calcium and iron) are present in (or on) zincate films. Some of these contaminants (i.e. sodium, chloride and iron) result from minor components in the proprietary zincating solutions. The others most likely resulted from inadvertent sample handling or from the adsorption of airborne contaminants prior to the analyses.

5. The zincate films prepared in this study were discontinuous as shown by SEM and the fact that small amounts of aluminium (oxide and metal) could be detected on the zincated discs by ESCA, ISS and SIMS.

6. ESCA results indicated that the composition of the zincate films prepared in this study consisted primarily of a $Zn(OH)_2$/ZnO mixture on the surface and zinc metal in the bulk of the film.

7. The complementary SEM, ESCA, ISS and SIMS results demonstrate the value and usefulness of these techniques for determining the effects of industrial processes on material surfaces.

References

1. G. O. MALLORY, *Plat. Surf. Fin.* **72** (1985) 86.
2. D. DIMILIA, J. HORKANS, C. McGRATH, M. MIRZAMAANI and G. SCILLA, *J. Electrochem. Soc.* **135** (1988) 2817.
3. M.J. PRYOR, *Oxid. Met.* **3** (1971) 523.
4. K. WEFERS, *Aluminium* **57** (1981) 722.
5. B. R. STRÖHMEIER, *Surf. Interface Anal.* **15** (1990) 51.
6. W. HANKE, H. EBEL, M. F. EBEL, A. JOBLONSKI and K. HIROKAWA, *J. Electron Spectrosc. Rel. Phenom.* **40** (1986) 241.
7. B. R. STROHMEIER, *J. Vac. Sci. Technol. A* **8** (1990) 3347.
8. C. D. WAGNER, W. M. RIGGS, L. E. DAVIS, J. F. MOULDER and G. E. MUILENBERG, (eds), "Handbook of X-ray Photoelectron Spectroscopy" (Physical Electronics, Eden Prairie, MN, 1979).
9. B. R. STROHMEIER, *J. Vac. Sci. Technol.* **A7** (1989) 3238.
10. *Idem, Appl. Surf. Sci.* **40** (1989) 249.
11. *Idem, Aluminium*, **67** (1991) 1209
12. B. R. STROHMEIER and D. M. HERCULES, *J. Catal.* **86** (1984) 266.
13. G. SCHÖN, *J. Electron Spectrosc.* **2** (1973) 75.
14. D. BRIGGS (Ed.), "Handbook of X-ray and Ultraviolet Photoelectron Spectroscopy" (Heyden, London, 1977).
15. C. D. WAGNER, L. H. GALE and R. H. RAYMOND, *Anal. Chem.* **51** (1979) 466.

Received 18 October 1991
and accepted 14 August 1992